Distribution Agreement

In presenting this thesis or dissertation as a partial fulfillment of the requirements for an advanced degree from Emory University, I hereby grant to Emory University and its agents the non-exclusive license to archive, make accessible, and display my thesis or dissertation in whole or in part in all forms of media, now or hereafter known, including display on the world wide web. I understand that I may select some access restrictions as part of the online submission of this thesis or dissertation. I retain all ownership rights to the copyright of the thesis or dissertation. I also retain the right to use in future works (such as articles or books) all or part of this thesis or dissertation.

Signature:

Morgan N. McCabe	Date

Understanding Interstellar Chemistry: A Look at Methanol Branching Ratios and the Search for Aminomethanol

By

Morgan N. McCabe
Master of Science

Chemistry

Susanna L. Widicus Weaver, Ph.D.
Advisor

Francesco Evangelista, Ph.D.
Committee Member

Michael Heaven, Ph.D.
Committee Member

Accepted:

Lisa A. Tedesco, Ph.D.
Dean of the James T. Laney School of Graduate Studies

Date

Understanding Interstellar Chemistry: A Look at Methanol Branching Ratios and the Search for Aminomethanol

By

Morgan N. McCabe
B.S., New College of Florida, 2014

Advisor: Susanna L. Widicus Weaver, Ph.D.

An abstract of
A thesis submitted to the Faculty of the
James T. Laney School of Graduate Studies of Emory University
in partial fulfillment of the requirements for the degree of
Master of Science
in Chemistry
2016

Abstract

Interstellar Chemistry: A Look at Methanol Branching Ratios and the Search for Aminomethanol

By Morgan N. McCabe

Understanding the complex chemistry of the interstellar medium (ISM) is a current challenge for astronomers and chemists alike. With nearly 200 species found thus far in the ISM, our understanding is growing; however, important questions remain. Among the species detected, methanol is a major species of interest due to its abundance in the ISM and the important radicals it produces upon photodissociation. Two major questions are: What are the branching ratios for the products of methanol photodissociation; and can glycine form in the interstellar medium? This dissertation reports on my current work and progress at attempting to answer these questions. First, I have searched for the rotational spectrum of aminomethanol, a believed glycine precursor. Second, I have studied photodissociation of methanol in an attempt to find the branching ratios for the formation of hydroxymethyl and methoxy radicals that have a large effect on complex organic molecule formation in the ISM.

Understanding Interstellar Chemistry: A Look at Methanol Branching Ratios and the Search for Aminomethanol

By

Morgan N. McCabe
B.S., New College of Florida, 2014

Advisor: Susanna L. Widicus Weaver, Ph.D.

A thesis submitted to the Faculty of the
James T. Laney School of Graduate Studies of Emory University
in partial fulfillment of the requirements for the degree of
Master of Science
in Chemistry
2016

Acknowledgements

My support was provided by Emory University and NASA Grant NNX15AH74G. I would like to thank Dr. Susanna Widicus Weaver for her amazing support and advising. I would also like to thank Dr. Michael Heaven and Dr. Francesco Evangelista for being members of my committee and for their help and feedback. I would like give a special thanks for Dr. Brian Hays who I worked with on the methylamine project and gave me advice on graduate school and lab. I would like to thank the Widicus Weaver research group with a special thanks to Luyao Zou and AJ Mesko for their help and encouragement. Thank to Sam Zinga for taking some additional data for the dark products of the the methylamine reaction and Elena Jordanov for her help sorting lines.

Contents

List of Figures

List of Tables

1 Introduction

1.1 Background

To date nearly 200 molecules have been found in the interstellar medium [1]. These molecules are made predominantly of hydrogen, carbon, oxygen, and nitrogen and are typically considered small by chemistry standards, usually containing anywhere from 2 to 13 atoms; those containing more than 5 atoms are referred to as complex organic molecules (COMs) [2]. Among the molecules found are common ones on Earth, such as methane, water, and ammonia. Due to the large differences in density and temperature along with the presence of high energy cosmic rays, many exotic, non-terrestrial species can be found such as radicals, ions, and isotopologues. One of the reasons there is so much interest in the interstellar medium is that it is postulated that early organic molecules on Earth came from extraterrestrial sources. The current thinking is that these molecules formed in interstellar clouds and became incorporated into comets or meteorites; which were then delivered them to the planet surface [3]. By studying the chemistry present in the interstellar medium, we can search for evidence of prebiotic molecules to understand the origins of life on our planet.

Radio telescope spectral observations are currently one of the major ways to determine which molecules are in the ISM. Taking the rotational spectrum of the ISM gives quantitative temperature and density information for each molecule (specifically those with a permanent electric dipole, and hence a rotational spectrum) since a rotational spectrum acts as a fingerprint of a given molecule's structure. This means that conformers, isotopologues, and vibrational states all contribute a unique set of rotational lines to the full spectrum. However, this also causes the spectra collected from the ISM to be quite complex. Considering the spectra taken from these radio telescopes often contain the rotational spectra of many different molecules, laboratory data are required for comparison. Thus an important part of studying interstellar chemistry is

obtaining laboratory rotational spectra of molecules believed to be in the interstellar medium, so as to be able to make confirmations of species straightforward.

1.2 Methanol in the ISM

Current understanding of interstellar chemistry is based around what is considered 3 phases of hot core/corino formation, when a molecular cloud starts to collapse, forming the beginnings of a star. Each phase produces a different "generation" of chemical species. In phase 1, simple molecules such as water, ammonia, and carbon monoxide are frozen on the surfaces of icy interstellar grains [4]. During phase 2, incident radiation photolyzes these species, creating radicals. Finally during phase 3, the system warms up as a star forms and these radicals are able to move across the ice surface and form larger, more complex organic molecules (COMs). As the ice grain continues to warm, the COMs leave the ice through desorption, and can go on to react in the gas phase.

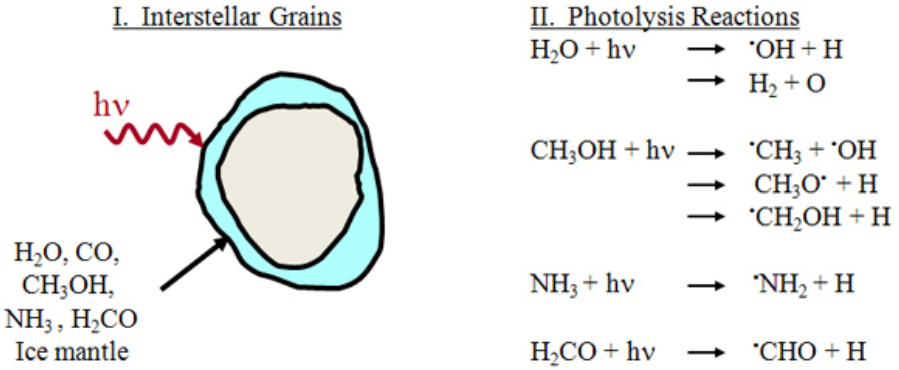

Figure 1: This figure illustrates the first two phases of ice grain chemistry that occurs in the ISM. Phase I shows the small molecules typically found on the ice mantle getting photolyzed and phase II shows the resulting photolysis products of these molecules.[4]

Methanol is important to study due to its high abundance, its ubiquitous nature, and its important photodissociation products. Methanol is among the more abundant interstellar molecules, both in the gas phase and on icy grains, with an abundance

ratio of 5 x 10^{-6} relative to H_2 in the gas phase, and 1% to 30% relative to H_2O ice in interstellar ice [2]. Additionally, in the ISM methanol is believed to be photodisscociated into three important products; hydroxymethyl (CH_2OH), methoxy (CH_3O), and methyl (CH_3) via the reaction mechanism below:

$$CH_3OH + h\nu \rightarrow CH_2OH + H \tag{1a}$$

$$\rightarrow CH_3O + H \tag{1b}$$

$$\rightarrow CH_3 + OH \tag{1c}$$

These radicals are important as they can then go on to react and form larger organic molecules such as acetaldehyde (CH_3CHO), glycoaldehyde ($HOCH_2CHO$), and methyl formate ($HCOOCH_3$):

$$CH_2OH + HCO \rightarrow HOCH_2CHO \tag{2a}$$

$$CH_3O + HCO \rightarrow HCOOCH_3 \tag{2b}$$

$$CH_3 + HCO \rightarrow CH_3CHO \xrightarrow[+OH]{-H} CH_3COOH \tag{2c}$$

As methanol is quite abundant, and these radicals are the basis for many of the more complex molecules that form, the photodisscociation branching ratios of methanol are important. The relative abundances of these radicals as well as their properties, such as how quickly they diffuse across the ice grain, are important for our understanding of ice grain and ISM chemistry.

Methanol photodissociation has been studied for over a century; the major dissociation pathways are given in the 5 channels listed below:

$$CH_3OH + h\nu \rightarrow CH_2OH + H \tag{3a}$$
$$\rightarrow CH_3O + H \tag{3b}$$
$$\rightarrow CH_2 + H_2O \tag{3c}$$
$$\rightarrow CH_3 + OH \tag{3d}$$
$$\rightarrow CH_2O + H_2 \tag{3e}$$

The first study conducted to measure the methanol photodissociation mechanism was by Fricke et al. [5] who found that formaldehyde was the major product. However, this study was flawed as it allowed time for the products to react and did not consider radicals. These flaws were remedied by Hagege et al. [6] where it was found that the hydroxymethyl and methoxy radicals were dominant products (75%) and formaldehyde was only a minor product (20%). More recently an experiment by Öberg and co-workers [7] studied the photolyzation of methanol in ices using IR and mass spectrometry, finding a branching ratio of 5:1:<1 for CH_2OH:CH_3O:CH_3 radicals. While this study is the closest to astrochemical predictions, an astrochemical modeling study by Laas et al. [8] showed that these ratios did not accurately predict the abundances needed for other molecules, such as methyl formate, to form. Additionally, studies up to this point have had difficulty determining the exact ratios of the hydroxymethyl and methoxy radicals because they cannot be distinguished using mass spectrometry. Lastly, a very recent study done in 2016 by Bertin et al. [9] used a quadrupolar mass spectrometer (QMS) to monitor the gas above a UV irradiated methanol ice. What they found was that when methanol ice was bombarded with UV radiation the methanol did not come off intact; instead CO was found to be the

predominant product though the reaction below:

$$CH_3OH_{(s)} + h\nu \rightarrow CO + 2H_2 \tag{4a}$$

This study adds to the previously established list of possible photodisscociation routes for methanol. CO was not previously considered in the methanol photodisscociation reaction scheme; however, in light of the latest study it is an important product, and may be detectable in low abundances due to its large dipole moment.

I have undertaken studies of the photodissociation branching ratios of methanol via rotational spectroscopy, which should allow us to determine the ratios of hydroxymethyl and methoxy using the methods described in the experimental section. This study is conducted in the gas phase and not on an ice grain surface, thus it will not be the exact conditions for methanol photodissociation that occur in the interstellar medium. However, studying the gas phase photodissociation has the ability to give two important results: (1) to find the rotational spectrum of hydroxymethyl which is not well determined, and (2) to get information on the branching ratios in the gas phase which is the simplest version of this system that can be studied, and may provide sufficient information for astrochemical models. This thesis covers some of the preliminary work done towards understanding the branching rations, including optimizing methanol depletion via laser photolysis as well as detecting a predicted product, formaldehyde, from this experiment.

1.3 Aminomethanol in the ISM

In addition to studying methanol photodissociation, I have focused much of my research on the search for prebiotic molecules of astrophysical interest. Aminomethanol is an important molecule in the interstellar medium as it is a possible precursor to biologically active molecules such as amino acids and sugars. Aminomethanol is be-

lieved to be formed from the radical reaction of hydroxymethyl (CH_2OH) and amidogen (NH_2) on icy grains. Aminomethanol is thought to be in the interstellar medium based on astrochemical simulations done by Charnley [10, 11] and Garrod et al. [4], but has not yet been detected. This is likely due to two reasons, the difficulty of analyzing observational data from the ISM, and the difficulty of getting a rotational spectrum of aminomethanol in the lab. Aminomethanol is an unstable molecule that is highly reactive in terrestrial conditions. A recent study by Feldmann et. al. [12] looked at the decomposition of aminomethanol to determine if it would be long-lived enough to observe in the interstellar medium. Its two dissociation routes are shown in Figure 2.

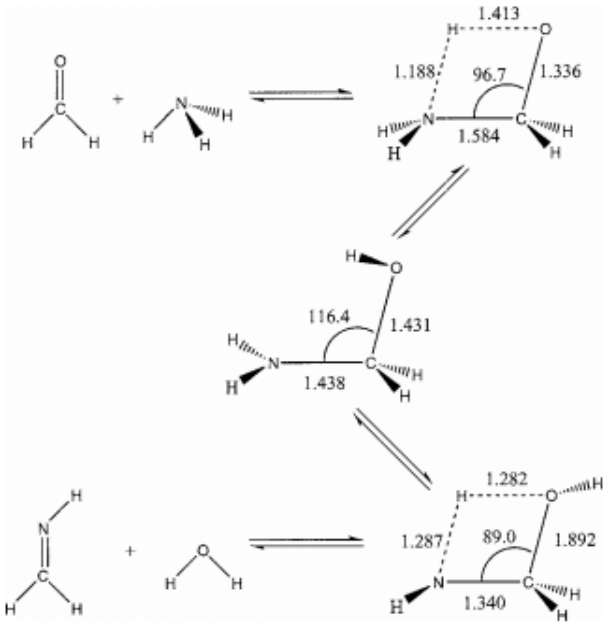

Figure 2: The decomposition routes for aminomethanol studied by Feldmann et.al. [12]

There has not been much previous work on aminomethanol, due to its instability under terrestrial conditions. A mechanism for forming aminomethanol in high enough abundance to be detected must therefore be developed before a laboratory spectrum can be obtained. Feldmann et. al. [12] suggested this species would be stable in

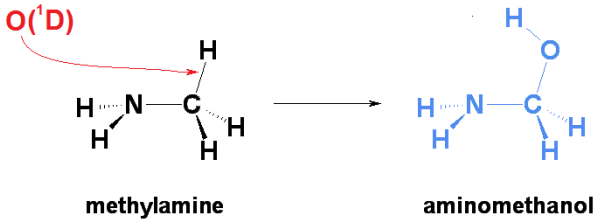

Figure 3: The mechanism of aminomethanol formation through insertion of O(^{1}D) into methylamine.

the interstellar medium, however the proposed mechanism for formation in the ISM is not easily performed in laboratory settings. For simplicity, O(^{1}D) insertion into methylamine was chosen as a method of making aminomethanol in the lab (Figure 3), as O(^{1}D) readily inserts into carbon-hydrogen bonds and the process is quite exothermic.

Previous studies have shown that O(^{1}D) readily inserts into methane to form methanol [13]; the formation of aminomethanol from methylamine is expected to be similarly exothermic [14]. This thesis continues work from Hays [13], extending the data collection to 302 GHz and sorting lines to simplify the search for the aminomethanol rotational spectrum.

2 Experimental

2.1 General Setup

Both the methanol photodissociation study and the aminomethanol study required the use of a direct absorption millimeter/submillimeter spectrometer and a laser photolysis source. The general experimental setup can be seen in Figure 4. For each experiment the molecule of interest was introduced into the system via gas lines backed with argon. From there the molecules were pulsed into a vacuum chamber using a pulsed valve, an externally timed valve that opens and closes using a solonoid

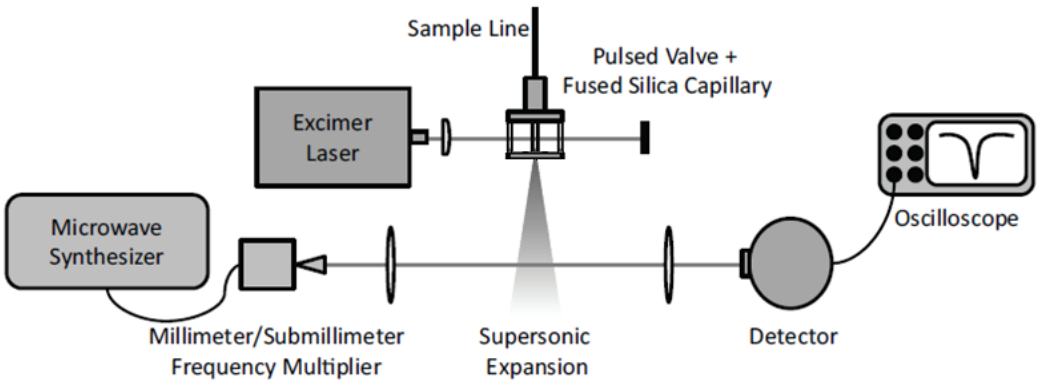

Figure 4: Experimental Setup. A 193 nm ArF eximer laser photolyzes the methanol in a fused silica tube and supersonically expands into a vacuum chamber, cooling the gas to 10 K. The molecules then pass through millimeter-wave beam and the rotational spectrum is taken with a bolometer and recorded using a digitizer card. Modified figure taken from Hays et al [14]

.

and springs to allow small amounts of gas through at set times and for a set duration. The difference between the high pressure gas behind the pulsed valve and the low pressure in the vacuum chamber allows for the molecules to supersonically expand once pulsed into the chamber, causing the molecules to be rotationally cold when probed spectroscopically. In addition, a fused silica tube was used in these experiments, placed directly after the pulsed valve, which enables a photolysis laser to interact with the sample. Once supersonically expanded into the chamber, the molecules and radicals formed from this process are detected, using millimeter/submillimeter direct absorption spectroscopy.

For both experiments, gas mixtures where delivered at a typical backing pressure of ∼1.2-1.34 atm; more information on the sample preparation for each experiment is given below. The gas mixture was pulsed through the fused silica tube and into the vacuum chamber using a pulsed valve (Parker Hannifan, Series 9). The chamber pressure was 15 mTorr which resulted in a supersonic expansion, cooling the gas to ∼10 K, as measured at a position of 5 cm from the nozzle. The 5 cm distance was chosen because it minimized overlap between the photolysis region and the mil-

limter/submillimeter beam, and yielded rotationally cold molecules within the zone of silence. The temperature was calculated via the rotational diagram method with methanol lines using the procedure described previously by Laas et al [15]. The fused silica tube (Wilmad Glass) was 3 cm long and had a 1 mm inner diameter. Molecules in the tube were photolyzed using UV light produced by an excimer laser (GAM Laser Inc. EX10) at either 193 nm for the methanol studies, or 248 nm for the O(1D) studies. After the tube, molecules passed through millimeter wave beam (20 GHz-1 THz) which was generated using an analog signal generator (Agilent Technologies, E8257D PSG with options 1EA, UNU, 550, and UNT) and multiplied to the correct frequency via Virginia Diode Inc. multiplier chains (Virginia Diodes Inc., AMC-S268). The rotational spectrum of the products was then recorded with a hot electron bolometer (QMC Ltd., QFI/XBI) after a single pass of light through the sample. The signal was then digitized using a National Instruments digitizer card (PCI-5124). Data was collected as a function of detector signal versus time, a time trace being collected at each frequency step. Having time, frequency, and intensity information allowed us to monitor reactant depletion/ laser product formation via molecular signal versus time as well allow us to see the relative intensity of lines at each frequency.

There were two methods of data collection used for these projects: point by point scans, and the fast sweep technique described in the paper by Zou et al. [16]. The fast sweep method uses triangle-wave modulation to make small frequency sweeps of about 6-9 MHz, depending on the multiplier chain, centered around the frequency of interest. These are averaged and saved and the frequency is then stepped to the next center point. This allows for broadband sweeps of 1 GHz to be taken quickly (about 30 minutes at 200 averages) allowing for more straightforward detection of unknown lines. Therefore, broad spectral searches were conducted using the fast sweep technique, and standard point-by-point frequency scans were used to confirm line positions, and acquire better signal to noise.

2.2 Methanol Experiment

For the methanol experiment, argon (NexAir, ultra-high purity) was bubbled through methanol at a backing pressure ∼1.48 atm. This mixture was then pulsed through a pulsed valve and into the fused silica tube, where it was photolyzed at a position 1 cm from the bottom of the tube, using a 193 nm ArF eximer laser (GAM LASER Inc. EX10) with an output power of 13.5 mJ. The expansion was probed with the millimeter/submillimeter spectrometer described above.

2.3 Aminomethanol Experiment

A similar set up was used for the methylamine O(^{1}D) insertion reaction. Methylamine (AirGas, 99%) was mixed with argon in a 1:3 ratio and run through the pulsed valve into a mixing block (Figure 6). This mixing scheme was used because previous attempts of mixing the methylamine and ozone without use of a mixing block allowed for substantial dark reactions to occur, causing a black goo to form which plugged the pulsed valve and precluded experiments. As a result, the mixing scheme was created to allow for as little mixing time as possible between ozone and methylamine.

From the primary pulsed valve, an ozone and oxygen (NexAir ultra-high purity) mixture was introduced into the mixing block. The ozone was produced from a Pacific Ozone L11 Ozone Generator, outputing 1% O_3 in O_2 at atmospheric pressure. A 248 nm KrF eximer laser was used to photolyze the ozone in the fused silica tube, forming O(^{1}D). O(^{1}D) was reacted with methylamine, which was delivered via the second pulsed valve at a pressure of 1.2 atm. The products were pulsed into the vacuum chamber at a pulse rate of 50 Hz and a duration of 2 ms. The expansion was probed with the millimeter/submillimeter spectrometer described above.

Additionally, a flow cell was designed by high school/undergraduate student Samuel Zinga in order to study the dark reactions of methylamine and ozone. Figure 6 shows

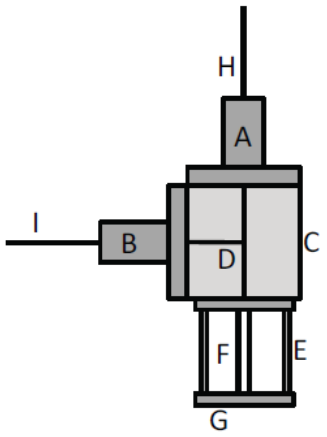

Figure 5: "A figure showing the mixing source comprised of the following: A) pulsed valve for ozone, B) pulsed valve for methylamine/argon, C) mixing block, D) gas channels, E) screws to hold the metal plate supports and fused silica tube in place, F) fused silica tube, G) mounting plate and output coupler, H) ozone gas line, I) methylamine/argon gas line." Figure and caption taken from Hays et al. [14]

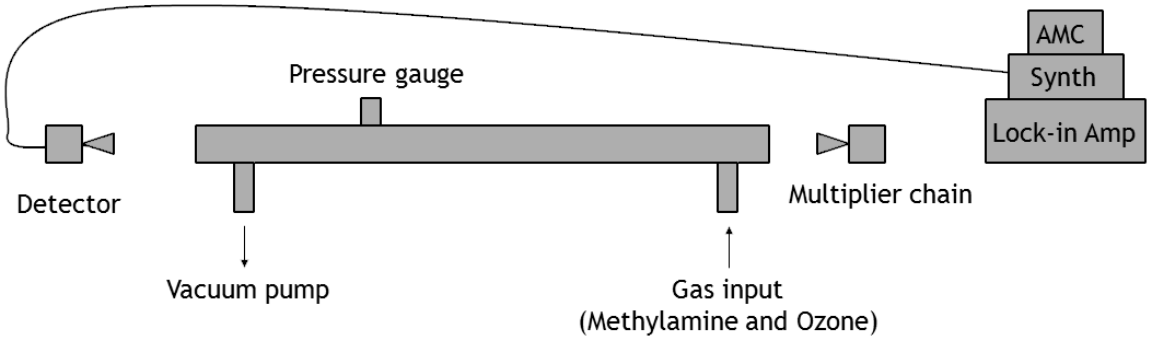

Figure 6: A schematic of the flow cell used to collect the spectra of the dark reaction between methylamine and ozone.

the design schematic for the flow cell. This flow cell differs from our lab's previous flow cells as it was made entirely of stainless steel rather than PVC in order to contain the methylamine safely during data collection. For this experiment, methylamine and ozone were mixed just before the flow cell and continuously flowed through the flow cell at a constant pressure of 50 mTorr. Spectra were collected from 140 GHz to 302 GHz using the same multipler chain and a zero bias detector (ZBD; Virginia Diodes WR5.1 53-23).

3 Methanol Results

Results for methanol photodissociation are shown in Figure 7. The first of these results showed that it was possible to photolyze methanol with the ArF 193 nm excimer laser. As can be seen in the figure, there is a methanol absorption peak which lasts from 500 μs to 1500 μs which is the duration of the open time for the pulsed valve. The laser RFI shows the time which the laser was fired during the pulsed valve being open, and the depletion in methanol immediately following this RFI spike suggests that methanol was photolyzed by the laser. Based on the terminal velocity of the gas mixture, it takes 49 μs for the molecules to travel from the end of the fused silica tube to where the millimeter beam passes (at a distance of 5 cm). Additionally, if the laser photolyzes methanol before the end of the tube it takes an additional 10 μs per cm to reach the millimeter wave.

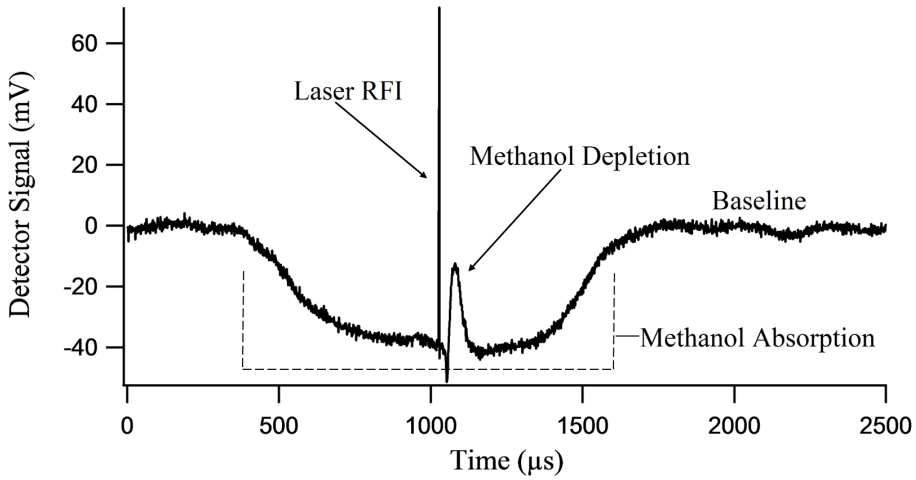

Figure 7: Preliminary results showing that methanol was photolyzed with the experimental set up. The large dip from ∼500-1500 μs is the methanol absorption peak. The laser RFI shows the time when the laser was fired, and at about 50 μs there is a depletion in the methanol signal due to it being photolyzed.

In addition to seeing evidence for the photolysis of methanol, the formaldehyde photoproduct was detected. Figure 8 shows the resultant formaldehyde lines detected between 140 and 220 GHz. Using the methods described in the Laas et al 2013 paper,

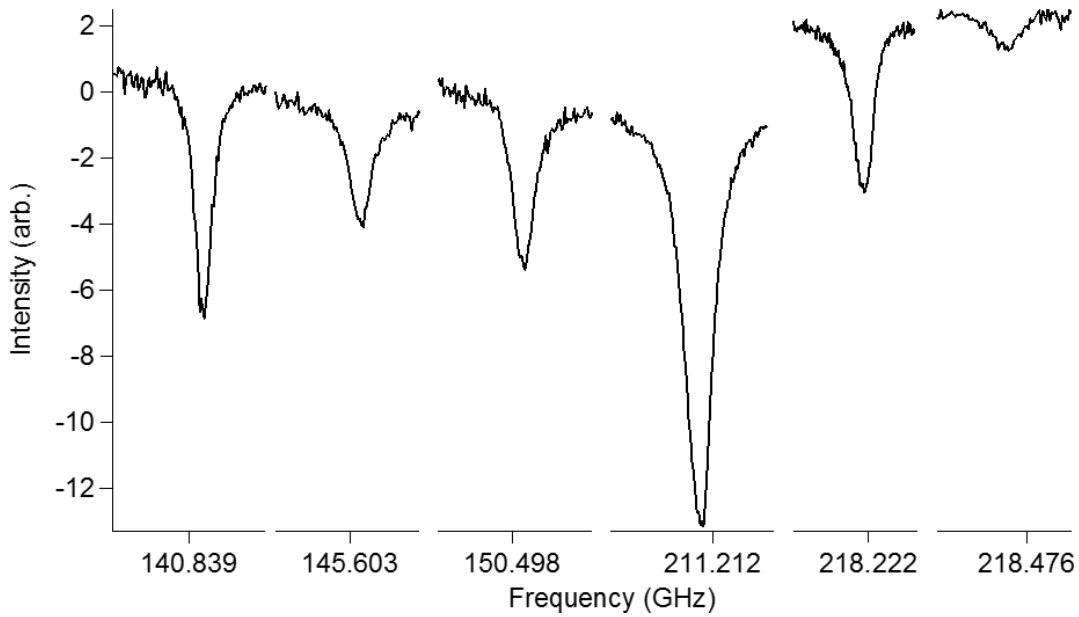

Figure 8: Formaldehyde peaks found from photolyzing methanol at 193 nm.

rotational temperatures and relative number density were found for formaldehyde and methanol; the associated rotational diagrams are shown in Figures 9 and 10. From these the rotational temperature of the molecules can be found from the inverse of the slope; for methanol, a rotational temperature of 24 $\pm$7 K was found, and formaldehyde was found to be at 16 $\pm$ 5 K. The intercept of these plots has a value of $\ln(N_T/Q(Trot))$, from which can be found the relative number density of formaldehyde produced from the methanol. The intensity for this experiment was not absolutely calibrated, thus true number densities cannot be determined from this experiment; however, the relative abundance of formaldehyde to methanol can be found. For this experiment it was found that formaldehyde is present at 0.0002% of the density of methanol.

One important note about the data shown above is that during the time this data was taken the laser beam was focused on the lowest part of the tube, the light illuminating the last third of the tube. This means that the formaldehyde seen is not likely the direct product of photolysis by the laser but rather the result of the

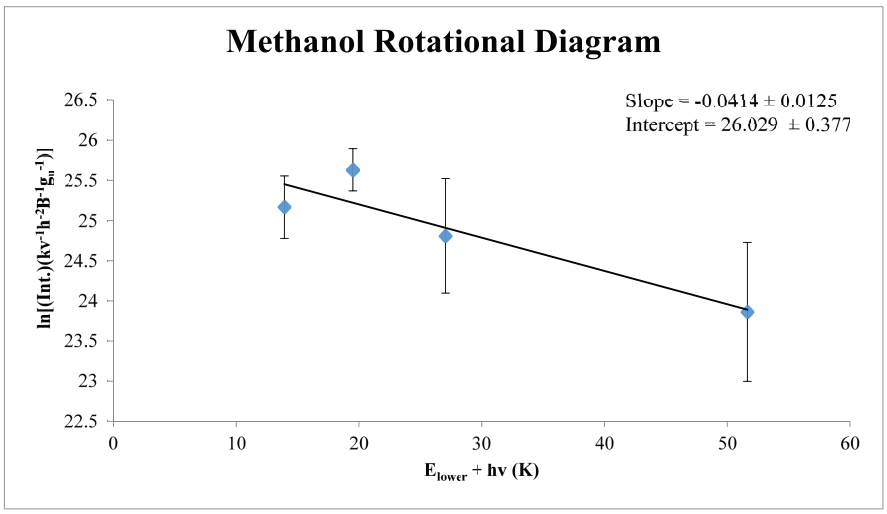

Figure 9: The rotational temperature diagram of formaldehyde, giving a temperature of 24 ± 7 K.

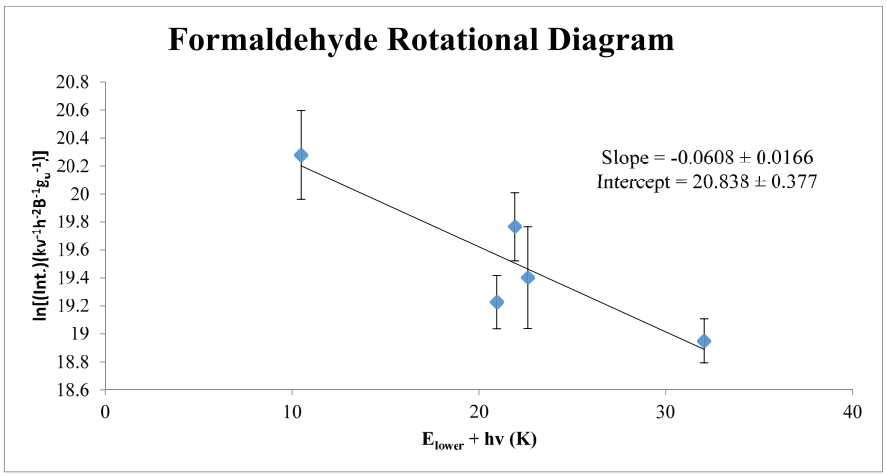

Figure 10: The rotational temperature diagram of formaldehyde, giving a temperature of 16 ± 5 K.

radicals formed at the bottom of the fused silica tube having some time to react within a closed area. Later studies within our lab have shown that the presence of formaldehyde decreases largely when the beam is placed below the tube, and with this depletion of formaldehyde the methoxy radical is able to be seen.

This work set the foundation for the branching ratio experiment and proves the system is effective for photolysis purposes. However, there is still much left to do as

detections of the methoxy and hydroxymethyl radicals are needed before any photodissociation branching ratios can be determined. The next step is to find methoxy lines, along with a number density and rotational temperature. Once methoxy is found, the next step is to do broadband sweeps to find the hydroxymethyl spectrum as it is not well determined. Finally, the fused silica tube needs to be removed to eliminate potential reactions before the photodissociation products are detected. It is unclear how removal of the tube will affect signal intensity, as the tube facilitates photodissociation because it guides precise laser alignment.

4 Aminomethanol Results

We have now collected 160 GHz of spectral data from 140-302 GHz to study the reaction O(^{1}D) and methylamine. Of this I was largely responsible for taking data in the range from 220-302 GHz (see Figure 8 and Appendix 1). This large range of spectral coverage was acquired quickly due to the use of the Fast Sweep technique discussed in Dr. Hays' dissertation [13], which allowed for broadband sweeps, sweeping through 6-9 MHz (depending on the multiplier chain) in steps, rather than single frequency point acquisition. The fast sweep was used as a broadband search tool to quickly find a large number of lines. From the data collected I then scanned through the spectrum and searched for lines which were then cross-referenced with a database of known rotational lines called Spalatlogue [17] to determine if they were known or unknown products.

Table 1 lists the products we were able to detect, those that we expected to see (but were not accessible in this frequency range), and those that were not detected. From this I was able to determine that there were 308 lines within this range not assigned to any molecule reported with previously recorded microwave spectra. In order to further narrow down possible candidates for aminomethanol lines, the total

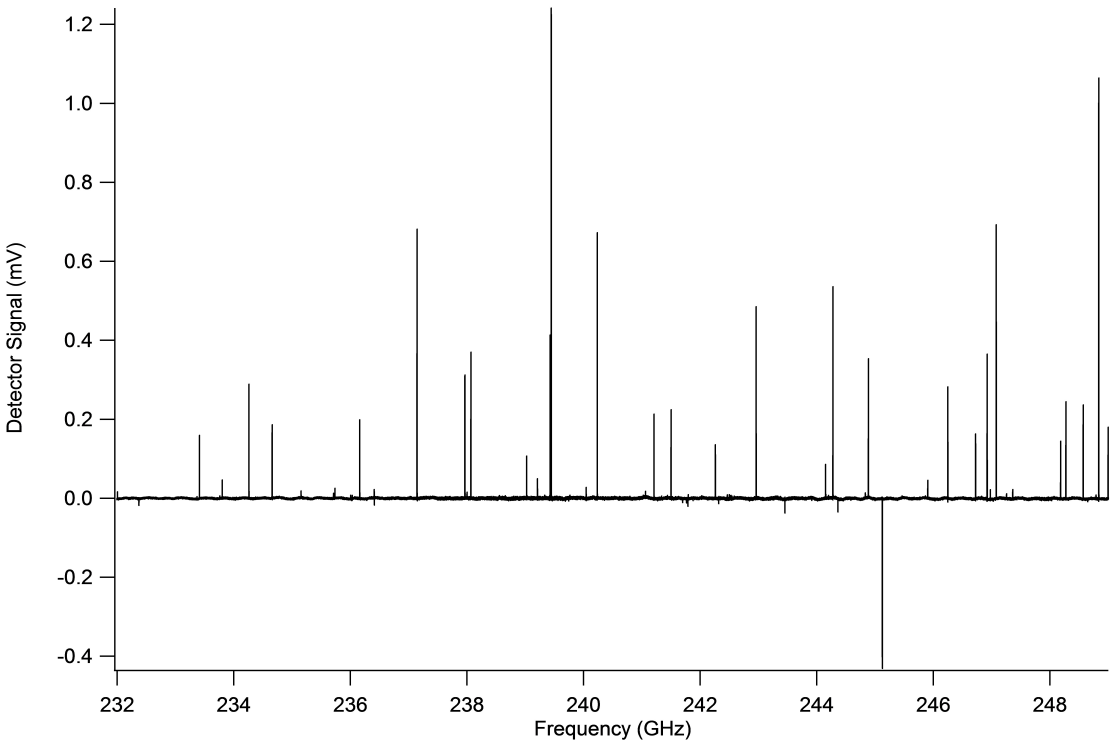

Figure 11: The spectrum taken using the fast sweep technique of methylamine + O(^{1}D) reaction from 232 to 250 GHz. The positive going peaks are dark products from the reaction of methyl amine and ozone, which are depleted when the laser is on. The down going peaks are laser induced products.

line list was further sorted into dark product lines and laser induced product lines. Dark product lines arise from the products of ozone and methylamine, in the absence of laser light. The first method used to sort the lines was using the single point scan method, using a 2D contour plot to view the molecular signal from these scans vs time. Typical results from this type of scan can be seen in Figures 12 and 13.

To determine laser induced vs dark product lines via this method, the laser spike at 50 μs was used as a time post to determine the presence of the signal. If the molecular signal was present prior to the firing of the laser, the product was already present and was thus a dark product. If the molecular signal only showed up after the time the laser was fired, then the line was then considered to be a laser induced product.

Table 1: The list of observed, expected, and not detected products found from the $O(^1D)$ experiment

Observed	Expected	Not Detected
$O_2(^1\Delta)$	CO	CN
NO	H_2O	HONO
HNO	NH_3	NH_2OH
HCN	OH	H_2CHOH
HNC		CH_3NHOH
HO_2		HOCN
NO_2		NH_2CN
H_2CO		HO_3
HOOH		
H_2CN		
HCNO		
HNCO		
CH_3O		
CH_2NH		
CH_3OH		
$HCONH_2$		

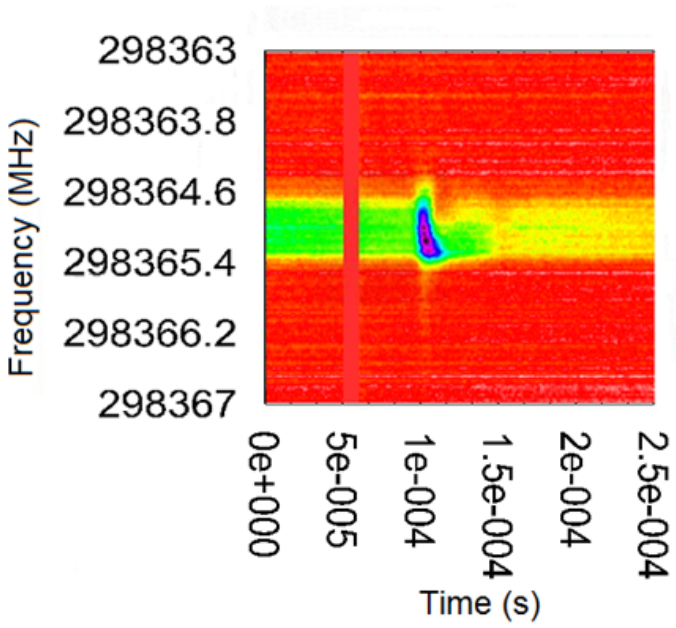

Figure 12: A 2D plot of a point by point scan of a dark product line. The time axis shows that the peak is present during the entire time of the experiment, before the laser fires at 50 μs. Intensity is given by color: red is low intensity, purple is high intensity.

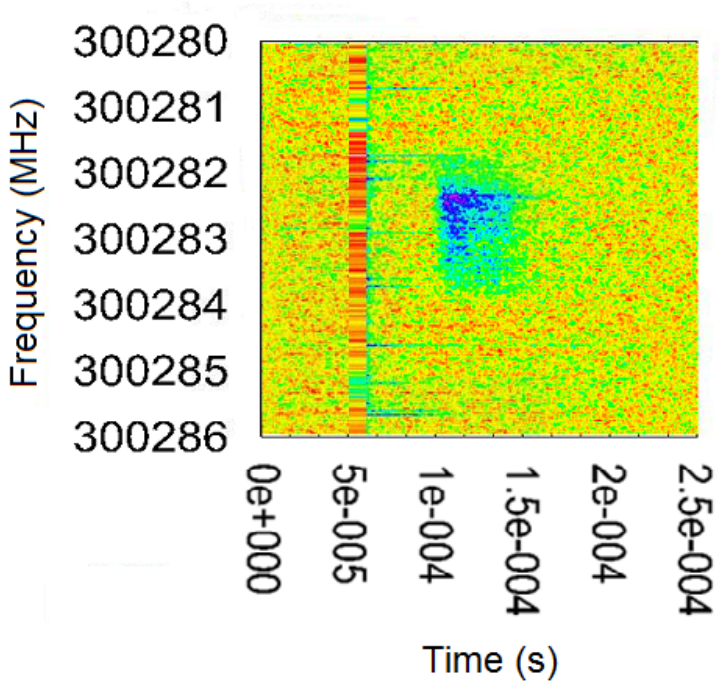

Figure 13: A 2D plot of a point by point scan of a laser induced product line. The time axis shows that the peak is present only after the laser fires at 50 μs. Intensity is given by color: red is low intensity, purple is high intensity.

Using the single point scan method was effective at determining what products were produced via laser photolysis; however, the process was time consuming using the single point scan method to revisit all 308 unknown lines, and a faster method was developed to sort the lines. Using the flow cell spectrometer developed by Sam Zinga, and described in the experimental section, the dark reaction between ozone and methylamine was studied directly, in the 140 to 302 GHz range. The recorded lines from the O(^{1}D) and methylamine experiment along with their intensities were then overlaid on top of the methylamine + ozone spectrum (Figures 14-16).

Using this method the unknown lines were compared to the dark product spectrum to see if they were present (see Figure 17). If present in the spectrum they were labeled a dark product; if not present, they were labeled a laser induced product. Using this method, the remaining unknown lines were sorted to laser induced and dark products; a list of lines is given in Appendix B.

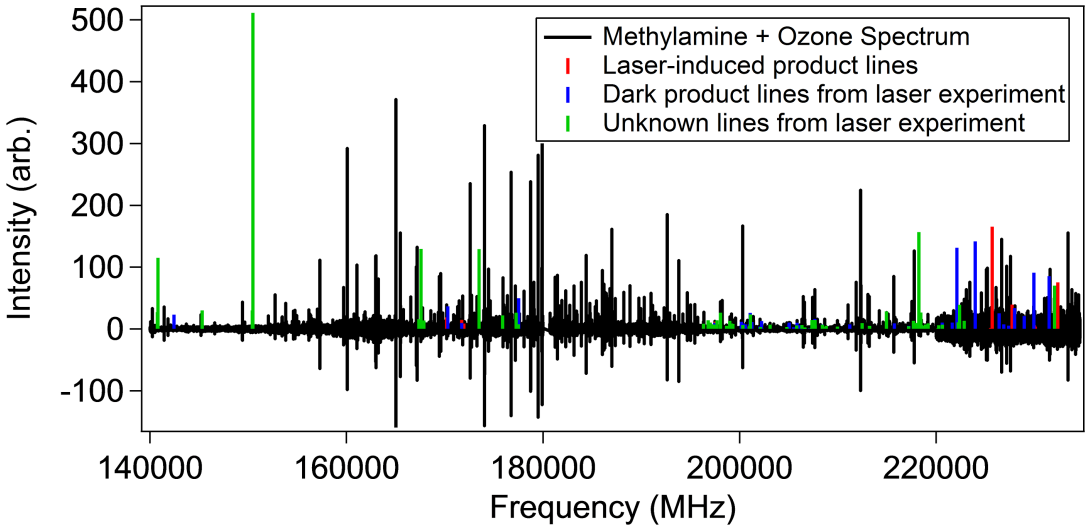

Figure 14: Unknown lines from the O(^{1}D) + methylamine laser experiment are overlaid on top of the spectrum of ozone + methylamine to help determine which lines arose from laser induced products.

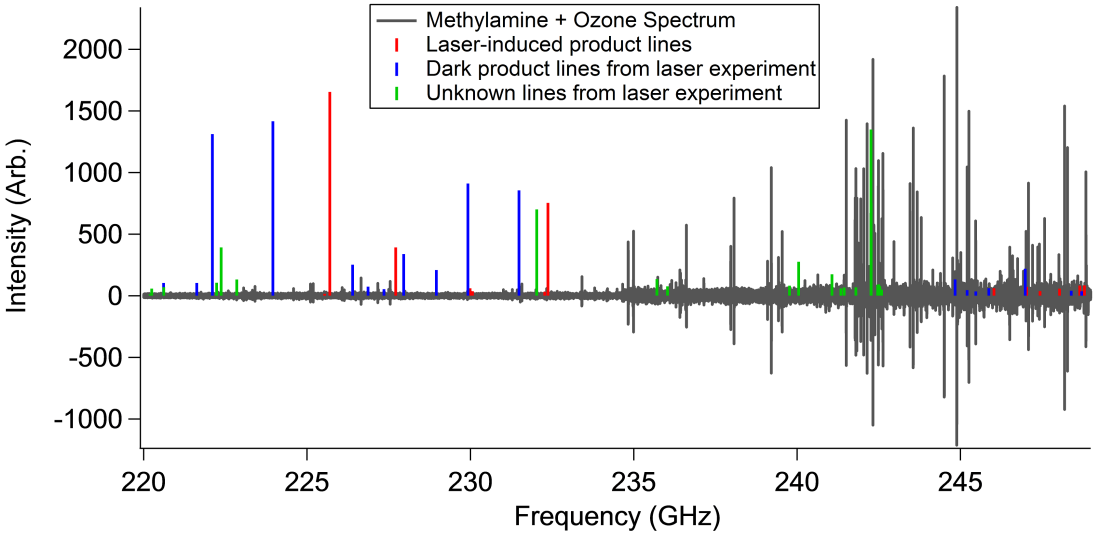

Figure 15: Unknown lines from the O(^{1}D) + methylamine laser experiment are overlaid on top of the spectrum of ozone + methylamine to help determine which lines arose from laser induced products.

Using this method the lines were narrowed down from 308 lines to 172 laser induced lines, helping to simplify the search for the aminomethanol. Thus far aminomethanol has not yet been confirmed, but additional analysis is underway. Some additional sorting has been performed looking at the known laser induced lines for the presence

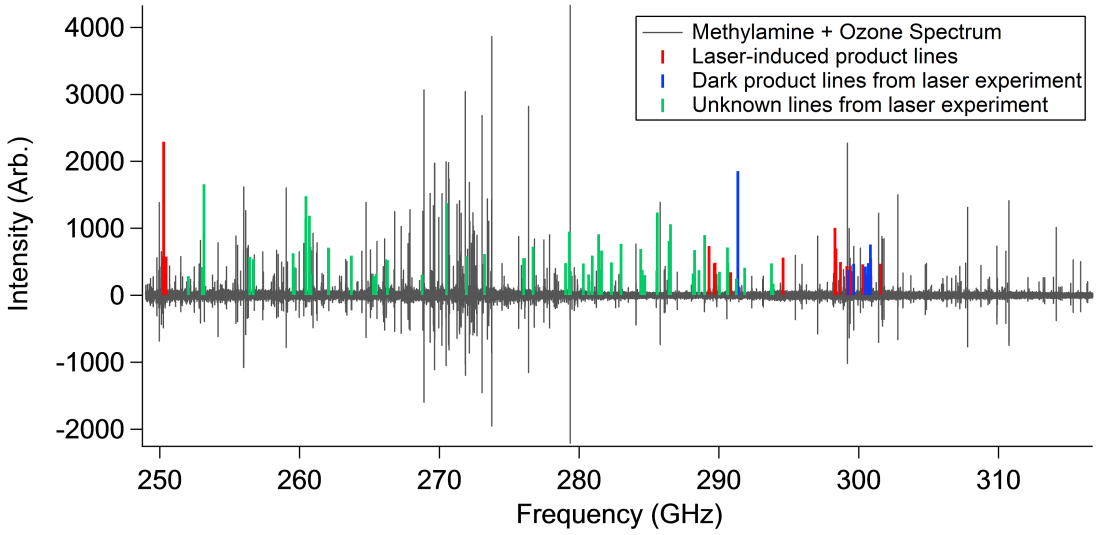

Figure 16: Unknown lines from the O(^{1}D) + methylamine laser experiment are overlaid on top of the spectrum of ozone + methylamine to help determine which lines arose from laser induced products.

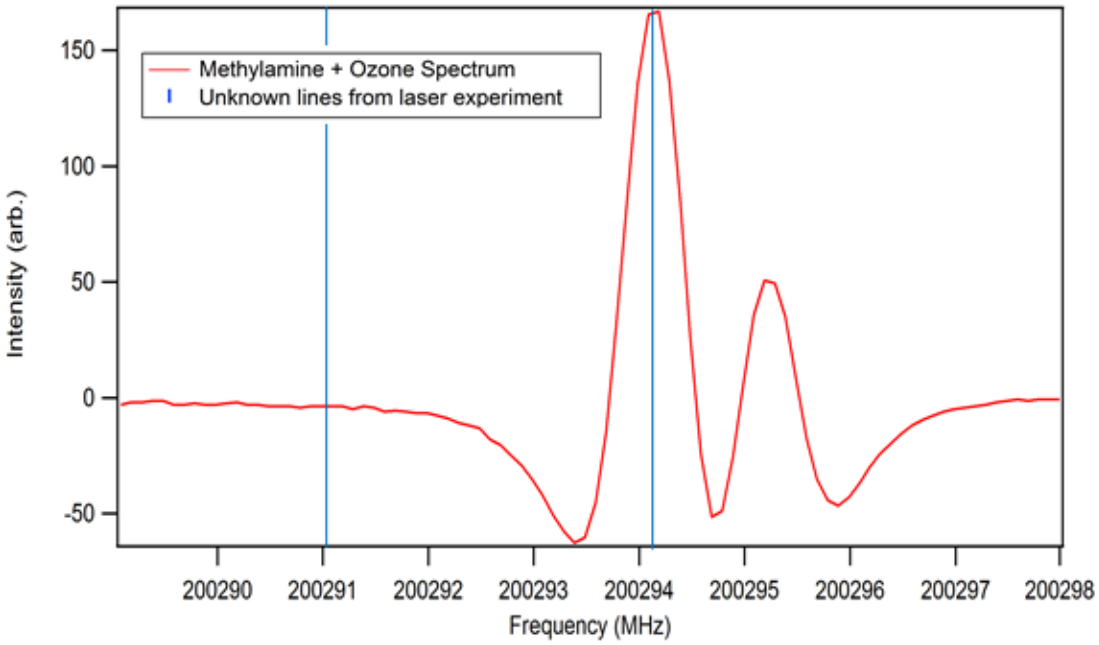

Figure 17: Two unknown lines from the O(^{1}D) + methylamine laser experiment are overlaid on top of the spectrum of ozone + methylamine to help determine what lines arose from laser induced products. The line on the left is laser induced as it does not appear in the methylamine + ozone trace.

of hyperfine splitting, as aminomethanol is nitrogen containing with a nuclear spin of 1. Figure 18 and Appendix C show potential line candidates for aminomethanol as these lines are both laser induced and hyperfine split.

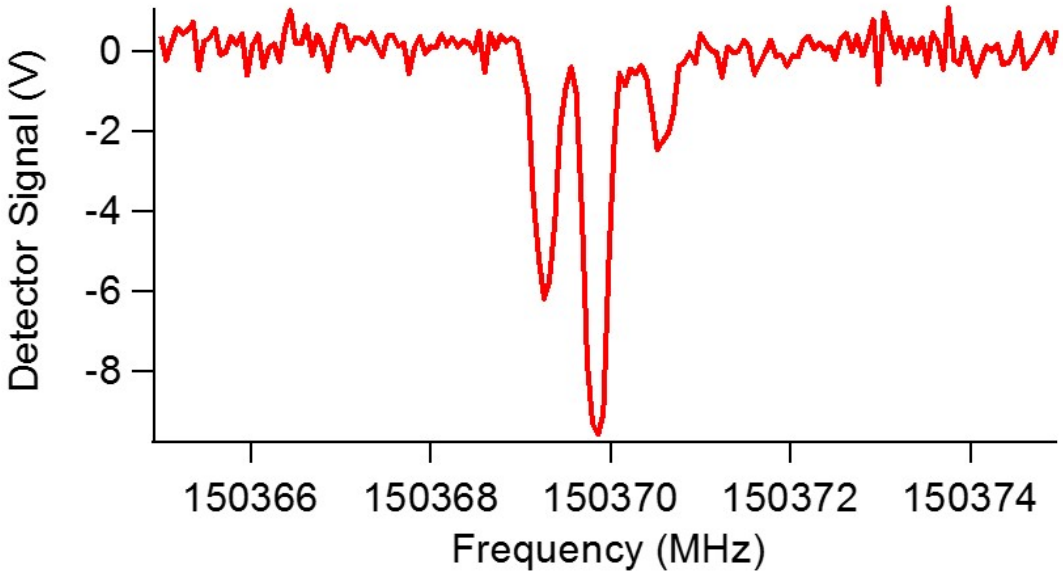

Figure 18: A potential aminomethanol candidate line that is both laser induced and displays hyperfine splitting.

As previously stated, based on the previous methanol studies we would expect that aminomethanol is a product and these unknown lines may be proof. However, analysis is still ongoing and there has been no successful fit of aminomethanol yet. It is expected that within the spectra we have collected there are aminomethanol lines, but the problem of identification it is quite complex and thus further analysis is needed. The difficulty in determining aminomethanol is due to the abundance of lines, having just narrowed down the possibilities to laser induced lines and further noting those with hyperfine. The next step for this project is to fit aminomethanol. Using the rotational constants calculated previously by Hays et al. [14] the rotational spectrum of aminomethanol was predicted at 15 K and compared to the known laser induced lines. There is not an obvious match between the two spectra, though this maybe

due to the experimental temperature of aminomethanol differing from predicted or additional spectral complexity arising from internal motion.

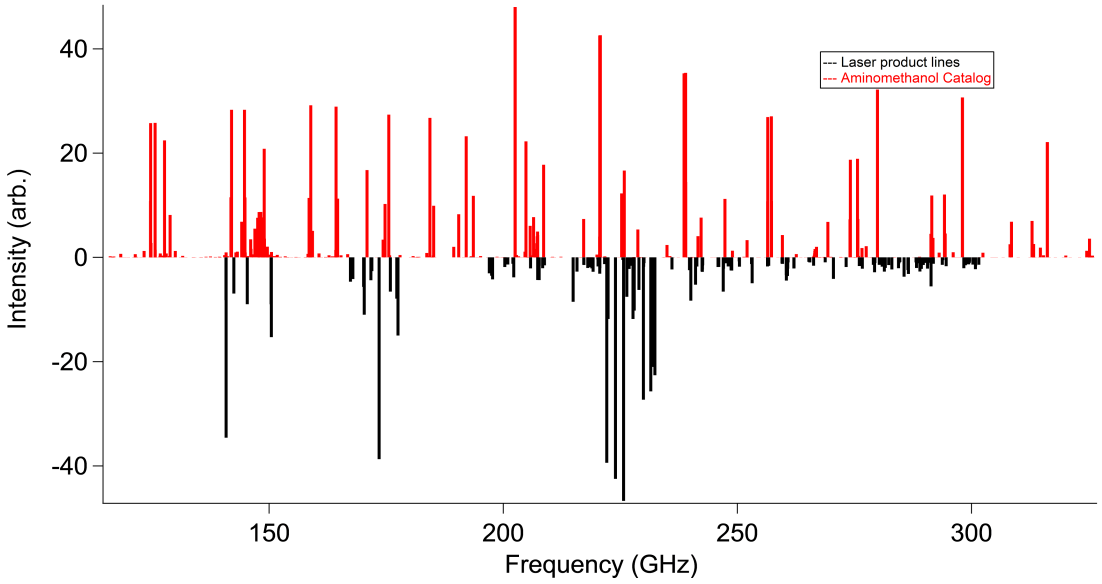

Figure 19: Laser induced lines found via experiment (shown in black trace) vs the predicted rotational lines for aminomethanol at 15 K (shown in red trace).

5 Conclusion and Future work

5.1 Methanol Photodissociation

Preliminary results from the lab for the photodissociation of methanol look promising, as I was able to photodissociate methanol with the laser rather easily. In addition, I was able to detect one of the many phototdissociation products expected, formaldehyde, and determine its rotational temperature and abundance relative to methanol. No other photodissociation products have yet been found, likely due to two factors: the methanol signal is not yet optimized, and the laser placement on the tube is hindering the formation or isolation of radicals. The chemistry of the expansion is very sensitive to the laser placement on the tube and during this experiment the laser was placed 1 cm from the bottom of the tube. It is therefore likely that the radi-

cals produced by photolysis reacted before they crossed through the millimeter beam. The most immediate course of action is to test what products can be detected based on where the laser photolyzes the methanol in the tube. As the radicals are quite reactive, the main focus would be on photolyzing close to the bottom and outside of the tube so as to reduce the time for the radicals to react before the expansion.

Work being done by new graduate student Carson Powers shows promise, photolyzing methanol entirely outside of the tube. From this there have been small amounts of methoxy produced, with only the strongest line in this range being observed. Future work for this project is to get a firm detection of the methoxy radical, along with rotational temperatures and relative abundances. Once that is complete, broadband sweeps should be performed both to see if there are any other products forming, as well as to better determine the rotational spectrum of hydroxymethyl, which is not well known. Finally, future experiments may search for the OH radical reaction path which is currently outside of our multiplier range. This can be remedied using deuterated methanol, as the OD radical has lines within our multiplier range.

5.2 Aminomethanol

Work has been done to detect the rotational spectrum of aminomethanol. Thus far is has not been confirmed, but spectra have been obtained, and much progress has been made in narrowing down possible candidates for aminomethanol lines. Now that the laser induced product lines have been identified, and these sorted into a list of lines that show hyperfine splitting, this can serve as a starting point for fitting aminomethanol. The next step for this project is to put the lines of interest into Autofit, a brute force triples fitting program [18] designed to make fitting spectra (especially those containing more than one molecule/conformer) easier. These lines of interest found will be a good starting point for Autofit, hopefully allowing us to get

the A, B, and C rotational constants so that we can compare to the aminomethanol prediction from theory.

Additionally when performing this search other lines without hyperfine will need to be considered as the hyperfine structure can collapse at higher J levels, making some of the broader laser induced lines also potential candidates. If additional analysis does not yield a reliable assignment for aminomethanol, more studies will be needed, experimenting with photolyzing in different spots in the fused silica tube to attempt to reduce the amount of dark products, or trying to repeat the experiment with fused silica tubes of differing inner diameters to promote aminomethanol quenching.

Appendices

A

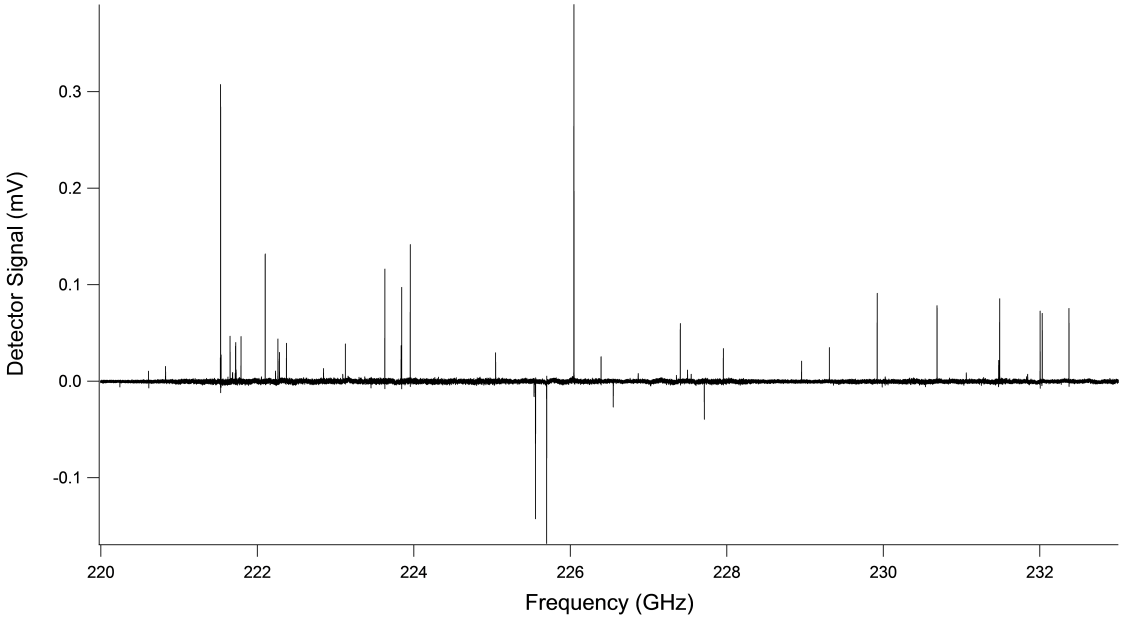

Figure 20: Spectral data from 260-302 GHz of the products of the O(^{1}D) and methylamine reaction

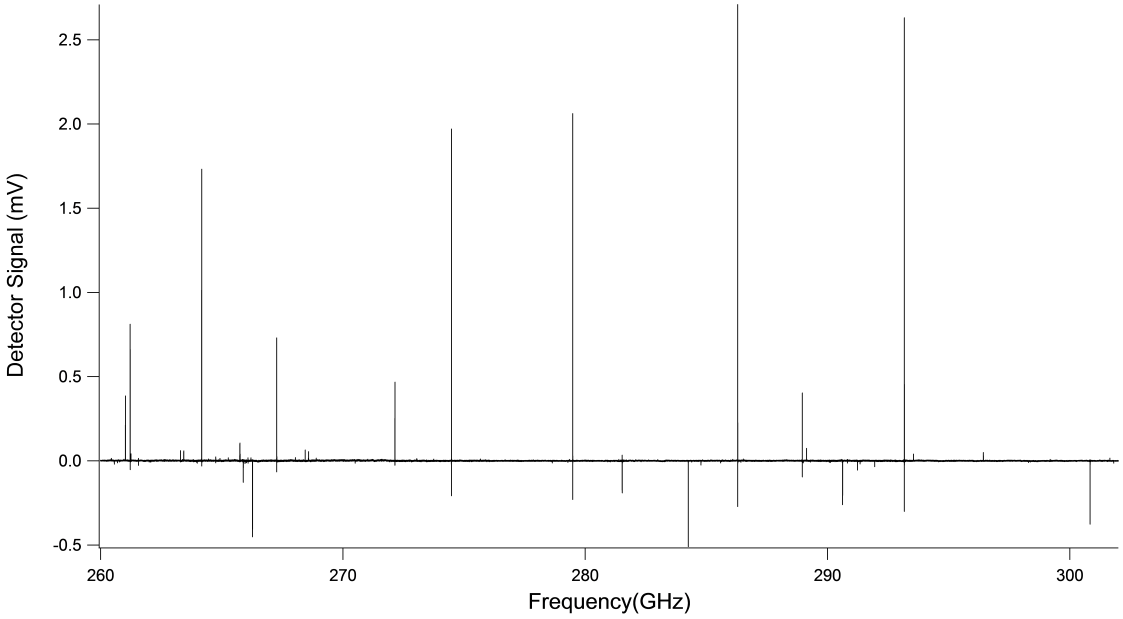

Figure 21: Spectral data from 260-302 GHz of the products of the O(^{1}D) and methylamine reaction

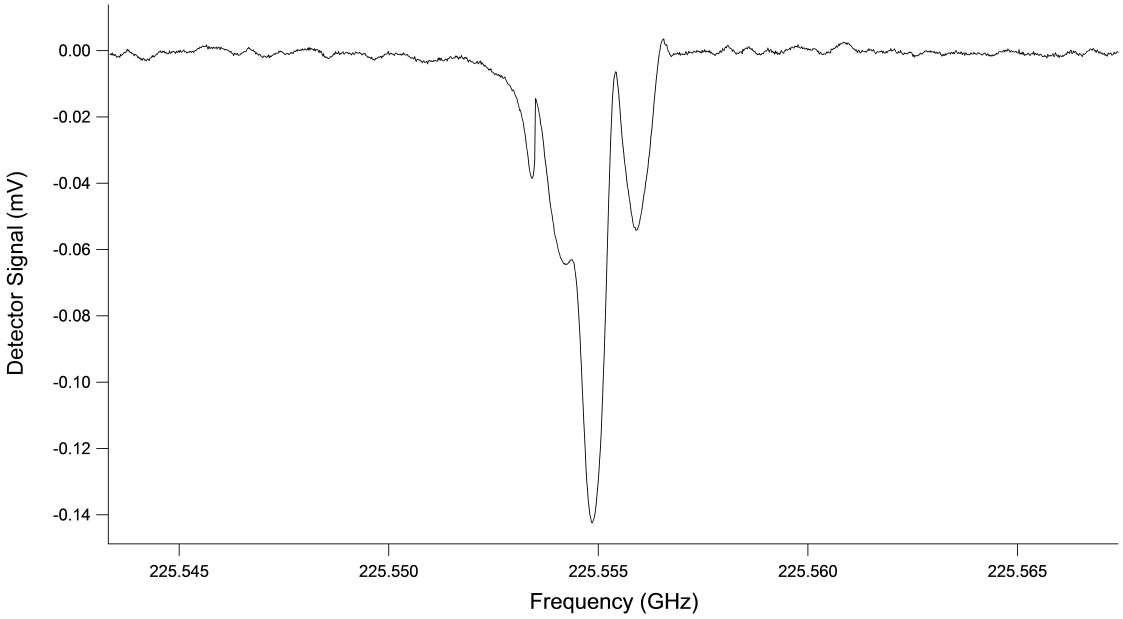

Figure 22: A laser induced product of methylamine and O(^{1}D) line with hyperfine splitting.

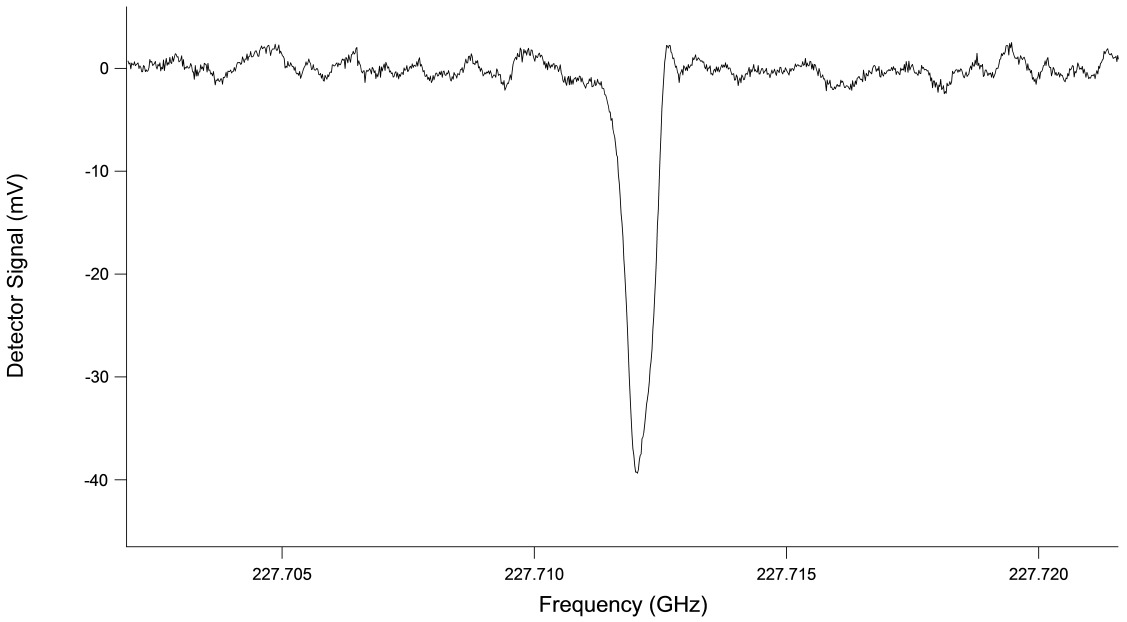

Figure 23: A laser induced product of methylamine and O(^{1}D) line without hyperfine splitting.

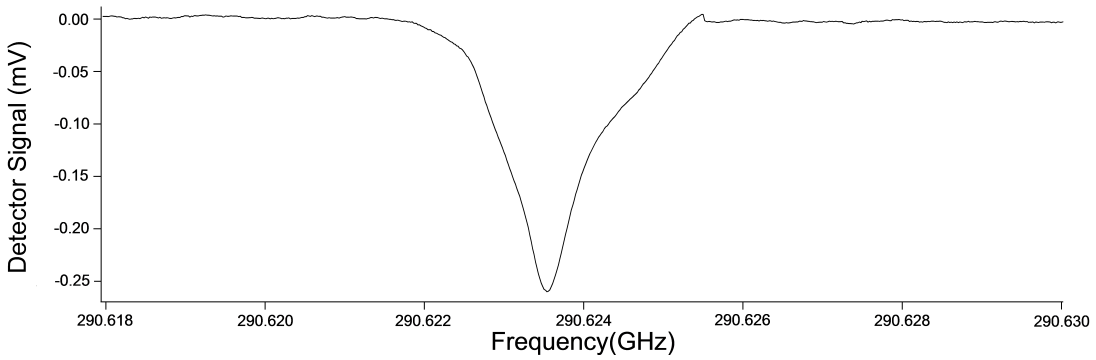

Figure 24: A laser induced product of methylamine and O(^{1}D) line that has hyperfine splitting, but is not fully resolved.

B

Table 2: List of current unknown lines from 130-302 GHz, sorted by type of product (laser induced, dark, or unknown), for the O(^{1}D) and methylamine experiment

Laser Induced	Dark	Unknown
170176.8	141386.8	134060
170177.5	142449.3	134178
171937.4	145994	134319
197508	170298.6	134616
197514	171714.7	134617
200291	177508.8	135293
200294	193643.8	135471
202104	197458	136173
202107	197483	137968
225536	197687	139513
225697.5	198043	140763.5
227712	198658	140807.5
229985.1	198975	145311.6
230059.9	198999	150418.2
232273.4	199170	150465.1
232372.5	200163	167356
246025.97	200166	167573
247026.01	200387	167871
247434.86	200390	173296.3
248029.12	200569	173485
248649.33	200572	175884.1
248658.48	200928	175884.2
248721.01	200931	177252.4

248792.56	200970	177266.8
250271.2	200973	177459.6
250391.57	200988	182638
250396.21	200991	183310
250436.66	201075	192906
250440.64	201078	193003
289000.66	201245	193796
289289.15	201248	196037
289655.13	202051	196040
289711.95	202054	196309
290837.16	202221.8	196790
294582.8	202289	197008
298292.1	205007	197321
298356.94	205031	197480
298365.06	205480	197517
298687.49	205815	197690
299149.18	205841	197698
299252.55	206121	198046
299394.33	206327	198661
299515.65	206623	198978
299567.58	206647	199002
300282.2	207104	199173
300540.59	207349	199299
300849.24	207403	199302
300858.33	207638	200321
301554.08	207641	200324
	207668	200972

	207670	201079
	207677	202106.8
	207678.52	203084.9
	207686.12	204808
	208407.16	205791
	208569.05	206330
	208682.56	206350
	208770.62	206626
	208788.96	206650
	208805.27	207101
	209962.05	207352
	211207	207381.5
	212454	207674
	213206	207678
	215732	207686
	217204.6	208407
	217759	208569
	219160	208770
	220608.7	208805
	221624.5	209949.1
	222100.2	212457
	223954	213205
	226392.6	213222
	226867.8	214927
	227355.37	217194
	227955.6	217194.7
	228955.5	217670

	229921.6	217764.2
	231487.2	217803.5
	244834.59	217830.5
	245201.56	217845
	245463.59	218014.7
	245862.51	218050.7
	246977.85	218223
	248388.37	218416.4
	248706.32	218460.9
	290616.37	218524.4
	291345.64	218578.3
	299221.72	218914.3
	299242.12	219152
	299637.02	219167
	300465.01	220196.7
	300685.1	220243.3
	300796.25	220613.2
	300814.34	222232
	300832.32	222372
		222845.9
		232030.5
		235709.87
		236031.01
		239765.16
		240046.21
		241062.84
		241338.96

		241438.64
		241797.09
		242261.65
		242465.23
		242499.91
		242521.12
		242528.55
		242547.13
		242583.8
		252029.3
		253027.01
		253152.46
		256424.98
		256683.95
		259529.94
		259639.18
		260433.15
		260433.15
		260446.8
		260461.14
		260695.75
		260745.74
		260810.56
		262057.02
		262074.11
		263692.51
		265273.34

			265475.94
			266281.88
			268762.84
			270506.56
			271926.39
			273223.4
			276023.69
			276691.06
			279027.86
			279282
			279284.9
			279377.1
			280291.58
			280678.62
			280910.3
			280930.76
			281385.94
			281462.29
			281594.83
			282303.46
			282995.13
			284395.37
			284500.78
			284690.08
			285588.24
			286425.12
			286526.55

		288141.43
		288248.8
		288568.28
		288966.91
		290035.5
		290597.4
		290605.39
		290642.29
		291245.62
		291834.25
		293751
		293871.33

C

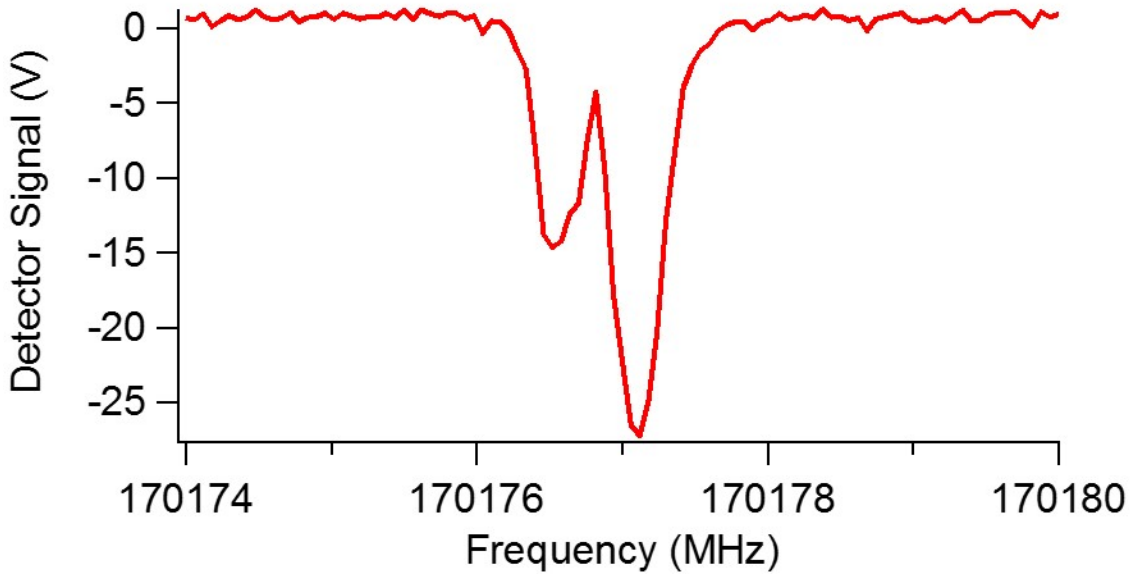

Figure 25: A potential aminomethanol candidate line that is both laser induced and displays hyperfine splitting.

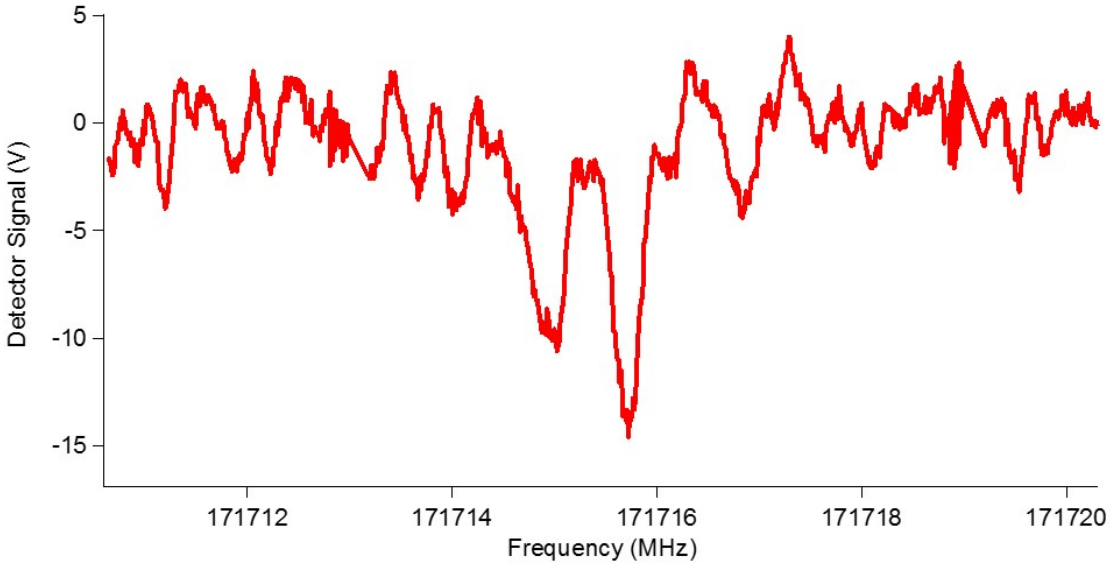

Figure 26: A potential aminomethanol candidate line that is both laser induced and displays hyperfine splitting.

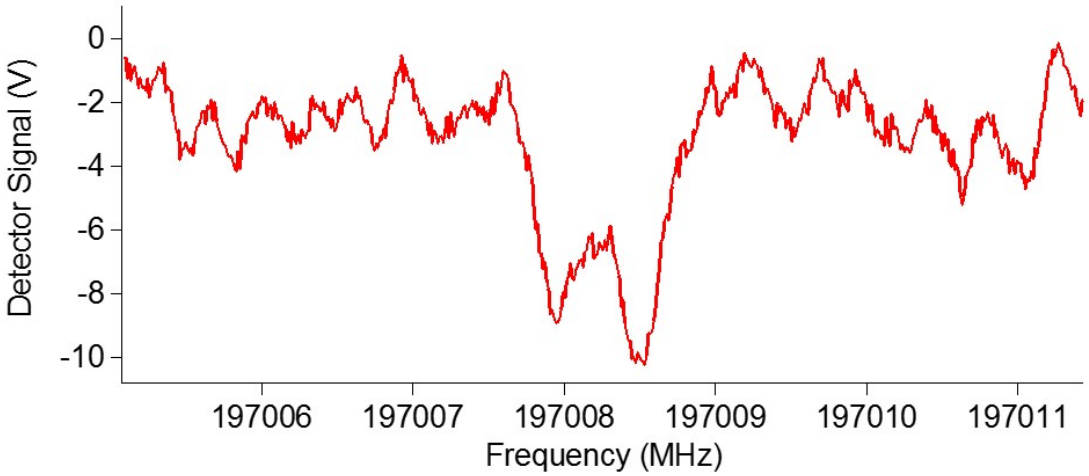

Figure 27: A potential aminomethanol candidate line that is both laser induced and displays hyperfine splitting.

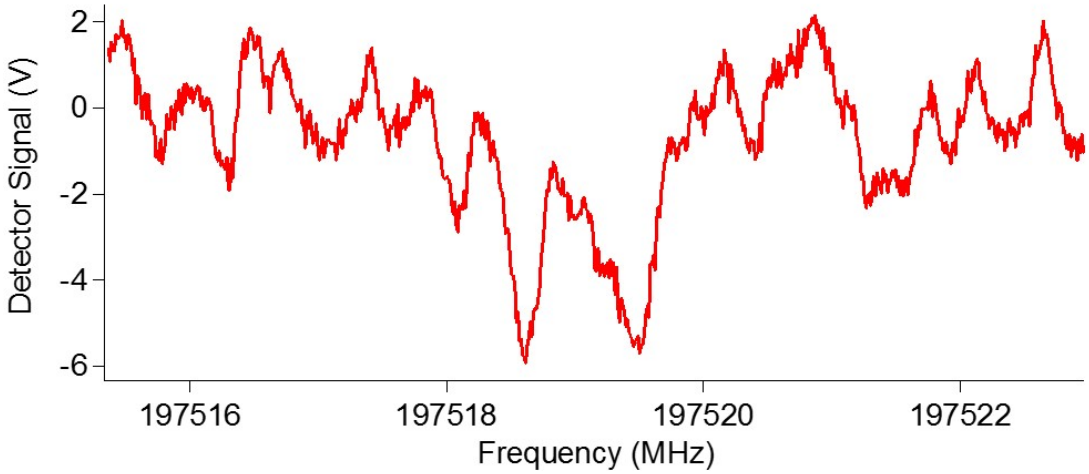

Figure 28: A potential aminomethanol candidate line that is both laser induced and displays hyperfine splitting.

References

(1) The Cologne Database for Molecular Spectroscopy Molecules in Space., `http://www.astro.uni-koeln.de/cdms/molecules` (accessed 10/17/2015).

(2) Herbst, E.; van Dishoeck, E. F. *Annual Review of Astronomy and Astrophysics* **2009**, *47*, 427–480.

(3) Albarde, F. *Nature* **2009**, *461*, 1227–1233.

(4) Garrod, R. T.; W. Weaver, S. L.; Herbst, E. *Astrophys. J.* **2008**, *682*, 283–302.

(5) Fricke, H.; Hart, E. J. *Journal of Chemical Physics* **1936**, *4*, 418–422.

(6) Hagege, J.; Roberge, P. C.; Vermeil, C. *Trans. Faraday Soc.* **1968**, *72*, 138–141.

(7) Öberg, K. I.; Garrod, R. T.; van Dishoeck, E. F.; Linnartz, H. *Astronomy —& Astrophysics* **2009**, *496*, 891–913.

(8) Laas, J. C.; Garrod, R. T.; Widicus Weaver, S. L. *Astrophys. J.* **2011**, *728*, 1–9.

(9) Bertin, M.; Romanzin, C.; Doronin, M.; Philippe, L.; Jeseck, P.; Ligterink, N.; Linnartz, H.; Michaut, X.; Fillion, J.-H. *The Astrophysical Journal Letters* **2016**, *817*.

(10) Charnley, S. B.; Rodgers, S. D. *Astrochemistry: Recent Successes and Current Challenges* **2005**, *231*, 237–246.

(11) Charnley, S. Interstellar Organic Chemistry., 2001.

(12) Feldmann, M. T.; Widicus, S. L.; Blake, G. A.; Kent David R., I.; Goddard William A., I. *Journal of Chemical Physics* **2005**, *123*, 034304–034304-6.

(13) Hays, B. Rotational Spectroscopy of O(^{1}D) Insertion Products., Ph.D. Thesis, Emory University, 2015.

(14) Hays, B. M.; Widicus Weaver, S. L. *Journal of Physical Chemistry A* **2013**, *117*, 7142–7148.

(15) Laas J. C., H. B. M.; L., W. W. S. *Phys. Chem. A* **2013**, *117*, 9548–9554.

(16) Zou L., H. B.; L., W. W. S. *J. Phys. Chem. A* **2016**, *120*, 657–667.

(17) National Radio Astronomy Observatory Splatalogue: database for astronomical spectroscopy., `http://www.cv.nrao.edu/php/splat/` (accessed 10/17/2015).

(18) Seifert, N. A.; Finneran, I. A.; Perez, C.; Zaleski, D. P.; Neill, J. L.; Steber, A. L., et al. *J. Mol Specrosc* **2015**, *312*, 13–21.